Progress In Electromagnetics Research M, Vol. 23, 123–137, 2012

A METHODOLOGY TO STUDY THE ELECTROMAGNETIC BEHAVIOR OF A CRYOGENIC METALLIC SYSTEM USED TO CONTROL THE RATCHET EFFECT

D. Medhat*, A. Takacs, and H. Aubert

CNRS; LAAS; 7 avenue du Colonel Roche, F-31077 Toulouse, France
University of Toulouse; UPS, INSA, INP, ISAE; LAAS; Toulouse F-31077, France

Abstract—We introduce an electromagnetic investigation of the complex experimental setup used in studying the Ratchet Effect at low temperature. This investigation, based on intensive electromagnetic simulations, shows that a compromise has to be taken into consideration between the physical aspects, the technological and the practical restrictions as well as the electromagnetic conditions of the observed phenomenon. By improving the electromagnetic response of the whole system, the Ratchet induced photovoltage can be increased, and hence the Ratchet device can be used for practical applications in wireless communications.

1. INTRODUCTION

Ratchet Effect [1] presents a very interesting physical phenomenon with exciting applications at the Nanoscale level. Recently, the Ratchet device has been proposed to be used in the fabrication of current generators and detectors at high microwave frequencies [2–6]; also with the possibility of using the terahertz radiation [9, 10]. The concept of operation [2–7] consists of radiating a two-dimensional electron gas asymmetric system with a microwave linear polarized radiation and producing a DC induced photovoltage. At low temperature, this effect is recently observed in AlGaAs/GaAs [2, 3] and Si/SiGe [4–6] heterostructure samples which are characterized by the high mobility of electrons. In order to generate the Ratchet transport in these samples, three conditions have to be satisfied. First condition is the

Received 6 December 2011, Accepted 23 January 2012, Scheduled 30 January 2012
* Corresponding author: Dina Medhat (dmedhat@laas.fr).

presence of spatial inversion asymmetry in the studied samples [1–15]. This can be achieved by patterning a periodic array of semi-discs shaped nanoantidots in a hexagonal lattice (using electron beam lithography) [2–6]. Second condition is the presence of a source of external energy which is represented by the microwave linear polarized radiation [2–8]. Finally, the third condition is that the period and the radius of antidots must be smaller than the mean free path of electrons at the working temperature [2–7], which is defined as the average distance covered by an electron between subsequent impacts. Realizing these conditions allows the collision of electrons with the antidots lattice and hence producing a directed electron motion in a certain direction and the restriction of motion in any other directions. As a result, a Ratchet directed transport of electrons has been observed and thus, an induced DC Ratchet photovoltage of few milli-volts has been measured between the sample contacts [2–6]. The fabrication of such a nanodevice represents a new and a challenging problem under the technology constraints.

For many years, the Ratchet phenomenon has been observed in various systems characterized by asymmetry and non-equilibrium including: (i) the biological molecular transport in systems such as proteins and bacteria [13]; (ii) the motion of liquid droplets on hot metallic asymmetrical surfaces [14] and (iii) semiconductor devices [15].

Another feature of the Ratchet Effect is that the directionality of the induced photovoltage could be controlled by the polarization of the microwave radiation. This feature has been predicted by theoretical studies [11, 12] and confirmed by practical experiments on AlGaAs/GaAs heterojunction samples [2, 3]. Recently, the dependance of the Ratchet photovoltage on the microwave polarization has not been observed in Si/SiGe heterojunction samples [5].

The Ratchet photovoltage has been measured at low temperature in CNRS-LNCMI, Grenoble, France [2–6]. A linear dependence has been noticed between the microwave power of the source and the photovoltage induced at a frequency around 50 GHz. The last magnetotransport measurements showed in [5, 6] are obtained using a large temperature range (1.4 to 77 K) and magnetic fields up to 15 T. These measurements have to be performed using a complex closed cryogenic metallic cavity system. Inside this closed metallic cavity, there is a complex metallic setup of various metallic shapes to support the sample, to rotate it in different angles and to connect it to the other instruments needed in measurements. Therefore, the presence of the cryogenic metallic cavity leads to the propagation of standing waves. Moreover, the other metallic parts inside of it disturb the electric field distribution. This makes the position of the sample inside the cryogenic

system very critical.

Our goal in this paper is to improve the Ratchet photovoltage by studying the electromagnetic response of the whole experimental setup used at low temperature. Due to the complexity of this closed setup, a methodology is proposed that helps in having a complete picture of the closed system used and hence improving its electromagnetic response. Several electromagnetic models have been created and simulated using full-wave electromagnetic simulation finite element method to represent the setup that could be used at room temperature [18–20] and the actual setup used at low temperature [16, 21]. Three descriptors have been computed that can quantify the Ratchet Effect inside the cryogenic system; the distribution of the electric field inside the cavity, the uniformity of the incident electric field linear polarization and the uniformity of the incident electric field density on the sample surface. Depending on the descriptors values and on the complexity of the actual setup, the best region where to put the sample inside the metallic closed cavity can be chosen which guarantees increasing the Ratchet photovoltage obtained. These descriptors have been calculated using HFSS full-wave electromagnetic simulator [17]. The results presented in [16] have been performed by using approximate dimensions of the experimental setup. However in this paper, the electromagnetic response of a realistic electromagnetic model of the experimental setup with the exact dimensions is presented.

We introduce, in Section 2, the methodology steps used in the investigation of the electromagnetic behavior of the whole system. A detailed description of the cryogenic closed metallic cavity system is presented in Section 3. In Section 4, there is an explanation of the various electromagnetic simulations models representing the front-end module of this closed setup. Finally, the electromagnetic response of each simulation model is discussed in Section 5.

2. METHODOLOGY STEPS TO INVESTIGATE THE ELECTROMAGNETIC BEHAVIOR OF THE EXPERIMENTAL SETUP

Here, we present the methodology steps that have been used to study the Ratchet Effect and to optimize the experimental setup from the electromagnetic point of view.

Step 1. A good understanding of the physical phenomenon and of the future applications based on it.

Step 2. Determination of the experiment conditions and studying the experimental setup used in observing the phenomenon.

Step 3. Developing simple electromagnetic simulations models of

the setup, and then increasing the complexity of the models structure to be as close as possible from the actual setup.

Step 4. Finding analytical equations that define the phenomenon thus enable us to enhance the system response.

This methodology can be applied to any studied phenomenon, in which there is a challenge between the physical and the electromagnetic experiment conditions. For example, in our case, using the closed metallic cavity of the cryogenic system and the microwave radiation are both essential to satisfy the Ratchet Effect conditions. But on the other hand, this cavity can impact negatively on the electromagnetic response of the whole system.

Step 1 was discussed in the introduction section, and the remaining steps are presented in the following sections.

3. DESCRIPTION OF THE EXPERIMENTAL SETUP USED AT LOW TEMPERATURE

The second step of the methodology is to have a good study of the experimental setup. This complex setup exists in CNRS-LNCMI and has been used in obtaining all the experimental results presented in [2–6]. The cryogenic system used is useful, from the physical point of view, as it gives a wide range of temperatures and magnetic fields. Figure 1(a) shows a photo of the whole system and Figure 1(b) is a schematic to clarify each part of the system. A tunable microwave carcinotron, in the 33–50 GHz frequency range, represents the source of the microwave linear polarization; and an attenuator is connected to the carcinotron output to control the signal level. A circular waveguide is used to guide the microwave radiation. A rectangular-to-circular waveguide transition connects the attenuator rectangular output to the circular waveguide input aperture. This circular waveguide penetrates the closed metallic cavity of the cryogenic system which allows keeping the semiconductor sample at low temperature.

The complex setup inside the cryogenic metallic cavity is shown in Figure 2. A second waveguide transition, circular-to-rectangular, is connected to the circular waveguide output aperture to focus the microwave energy on the rectangular sample. The rectangular aperture of the transition is a WR22 with 5.69 mm length and 2.84 mm width. The sample lies in a ceramic package and its contacts are connected to the package contacts using wire bonding. There are some copper wires which connect the package contacts to the pins of three other black packages and finally to a thermal resistance. The aim of this thermal resistance is to indicate the temperature inside the closed metallic cavity. These copper wires are also connected to a voltmeter, digital

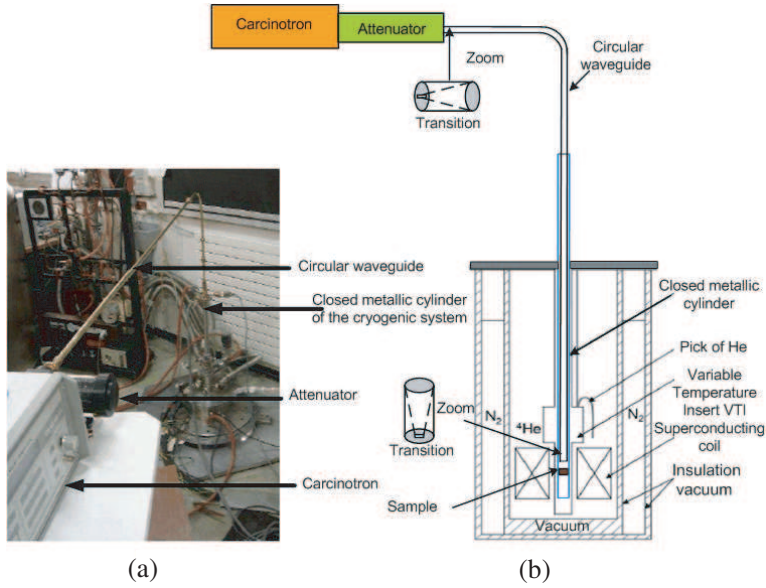

Figure 1. (a) Photo [2] of the complete experimental setup. (b) Schematic of the setup showing the different parts of the cryogenic system used.

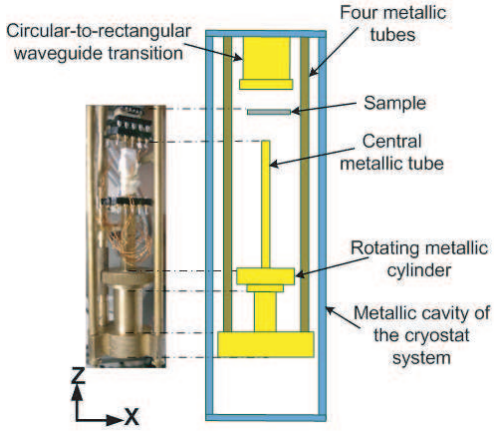

Figure 2. Photo and schematic of the complex metallic setup inside the metallic cavity of the cryogenic system.

multimeter with high accuracy, to measure the photovoltage produced between each two contacts of the sample. At the center of the metallic cavity, there is a metallic tube that holds the sample and the packages. Under this central metallic tube, a rotating metallic cylinder permits to

rotate the sample 360 degrees and hence changing the direction of the sample with respect to the direction of the microwave field. Another four metallic cylindrical tubes are placed near the boundary of the metallic cavity.

4. ELECTROMAGNETIC SIMULATION MODELS REPRESENTING THE FRONT-END MODULE OF THE EXPERIMENTAL SETUP

Now, the third step of the methodology consists of modeling the front-end module of the setup. As described in Section 3, in order to keep the sample at low temperature, a closed metallic cavity is used. The presence of this metallic cavity leads to the propagation of standing waves inside of it. Moreover, the complex setup inside of the cavity and its various metallic parts has a great influence on the distribution of the microwave field. Thus, the presence of the metallic closed cavity, as well as, the complex metallic setup inside of it, makes the choice of the sample position very critical.

Many simulation models, sketched in Figure 3, have been designed using the full-wave Ansoft HFSS software. Model 0 represents the simplest case of the hollow metallic cavity. The radius of the cavity is 14.205 mm, so by using a Matlab code, the number of modes inside the cavity is found to be 58 at the operating frequency of 50 GHz. Afterwards, a series of models have been simulated; Model 1, Model 2, Model 3 and Model 4; in each one a metallic part has been added to be as close as possible from the actual setup. The height of the cavity is taken to be 179.62 mm which corresponds in the actual setup to the distance from the output aperture of the circular-to-rectangular waveguide transition till the bottom of the metallic cavity. Except for Model 3 and Model 4, where a distance of 20 mm has been added to the height of the cavity. This additional distance represents the penetration height of the waveguide transition into the cavity. A wave port has been used to represent the source of the microwave energy with the same dimensions of the WR22 presented in the previous section. To symbolize the sample, many rectangles with a surface of $4\,\text{mm} \times 2\,\text{mm}$, have been placed at different positions inside the cavity. They have been put in the common area between all the models, near the output aperture of the waveguide transition. These simulation models have been split using one symmetry plane: perfect magnetic boundary conditions (y-z plane), to reduce the calculation simulation time.

HFSS software is used to simulate these models, as it includes a field calculator that enables us to calculate the analytical equations,

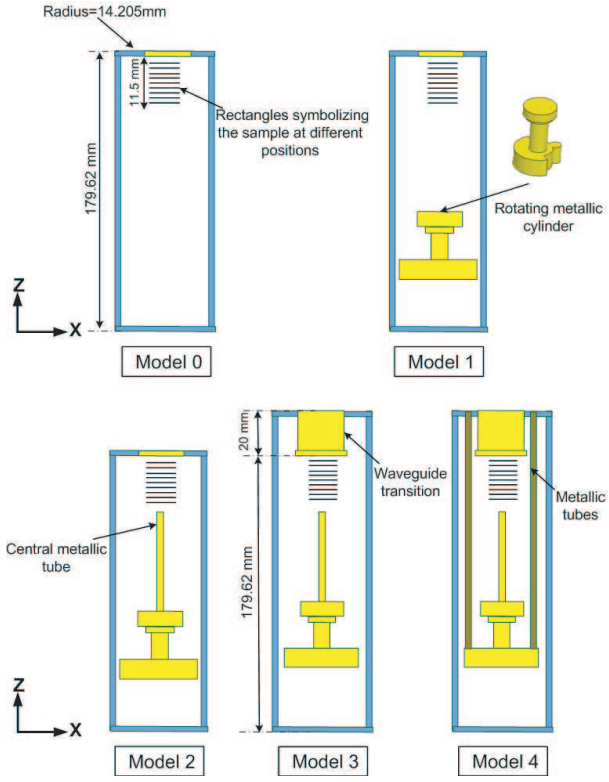

Figure 3. Schematics of the simulation models representing the front-end module of the experimental setup.

presented in the next section, which quantify the Ratchet Effect. But according to the setup dimensions, there is a challenge in simulating these very big structures using the finite element method which requires a huge computation time and large memory.

5. STUDYING THE ELECTROMAGNETIC RESPONSE OF EACH SIMULATION MODEL

In this section, the fourth step of the methodology is presented which requires an analysis of each simulation model response. This analysis is based on electromagnetic analytical equations that define the Ratchet Effect in a simple manner. This allows us to determine two important parameters of the Ratchet Effect: the amount of the incident electromagnetic field on the sample surface and the effect of

the electric field polarization.

i. Studying the distribution of the y-component of the electric field E_y inside the metallic cavity. As mentioned in Section 4, standing waves are observed in the closed metallic cavity. As a result, some regions with maximum values of the electric field and others with zero fields are found inside the cavity. Thus, the distribution of the electric field has to be studied to make sure that the sample is in a position where there are high values of the electric field y-component to produce the Ratchet photovoltage. This distribution changes each time a metallic part is added to the simulation model.

ii. Calculating the uniformity of the electric field linear polarization on the sample surface using 1.

$$K_E = \min^R \frac{\left|\vec{E_y}\right|}{\left|\vec{E_t}\right|} \times 100[\%] \tag{1}$$

$|\vec{E_y}|$ is the magnitude of the electric field y-component vector and $|\vec{E_t}|$ is the magnitude of the total electric field vector. When the electric field is oriented along the y-axis, it forces the electrons to oscillate vertically and scatter with the semicircular side of the antidots. This leads the electrons to move to the right and hence producing a photovoltage. Thus in this equation, we compare the value of $|\vec{E_y}|$ with respect to $|\vec{E_t}|$ on the sample surface. If K_E increases, this signifies that $\vec{E_y}$ is the major component of the electric field on the surface and that the electric field linear polarization is uniformly distributed on the overall sample surface to generate the Ratchet Effect. Moreover, in the piratical experiments, the sample is rotated 90 degrees to study the influence of the microwave polarization on the direction of the induced photovoltage in AlGaAs/GaAs and in Si/SiGe samples. This descriptor can also be used in this polarization study by replacing $|\vec{E_y}|$ by $|\vec{E_x}|$ in the above equation.

iii. Calculating the uniformity of the y-component of the electric field density on the sample surface using 2.

$$K_D = \frac{\min^R \left|\vec{E_y}\right|}{\max^R \left|\vec{E_y}\right|} \times 100[\%] \tag{2}$$

When comparing between the minimum and the maximum values of the electric field y-component on the overall sample surface, we can test the uniformity of the electric field density. If K_D increases, this signifies that there is no large difference between the minimum and the maximum values and that the y-component of the electric field density

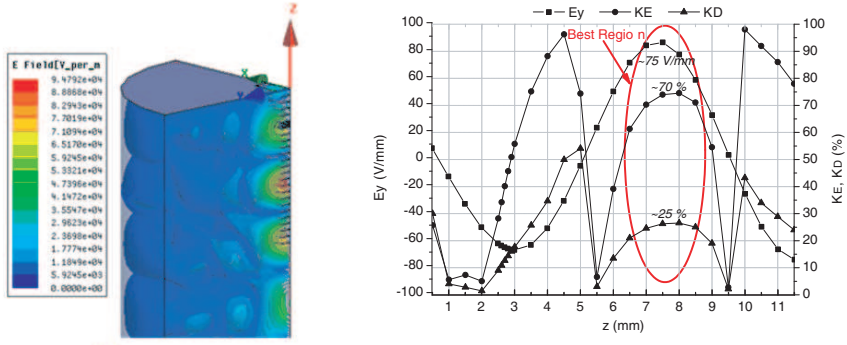

(a) (b)

Figure 4. (a) 3D plot of the magnitude of the total electric field in V/m inside the closed metallic cavity. (b) E_y, K_E and K_D calculated on the rectangles representing the sample at different positions (Model 0).

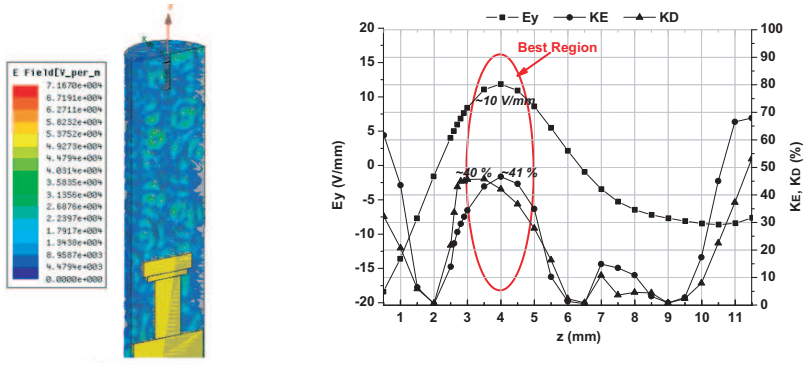

(a) (b)

Figure 5. (a) 3D plot of the magnitude of the total electric field in V/m inside the closed metallic cavity. (b) E_y, K_E and K_D calculated on the rectangles representing the sample at different positions (Model 1).

is uniformly distributed on the sample surface hence producing high values of the induced photovoltage.

Equations (1) and (2) have been computed using the field calculator of HFSS, on rectangles R which have the same dimensions of the real sample (4 mm × 2 mm). These rectangles are at a distance of 0.5 mm to 11.5 mm from the wave port for Model 0, Model 1 and Model 2. But for Model 3 and Model 4, this distance is measured from the transition output aperture.

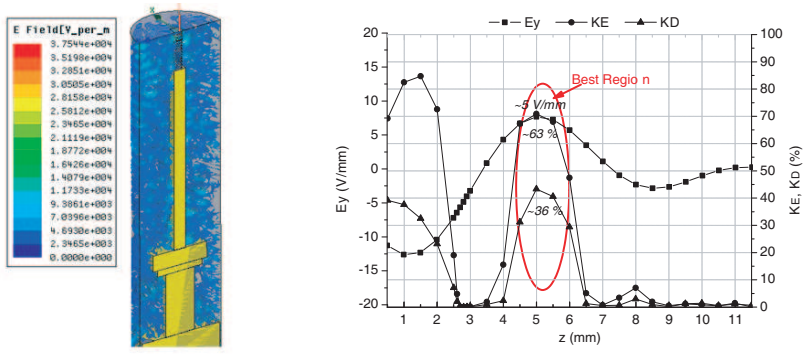

(a) (b)

Figure 6. (a) 3D plot of the magnitude of the total electric field in V/m inside the closed metallic cavity. (b) E_y, K_E and K_D calculated on the rectangles representing the sample at different positions (Model 2).

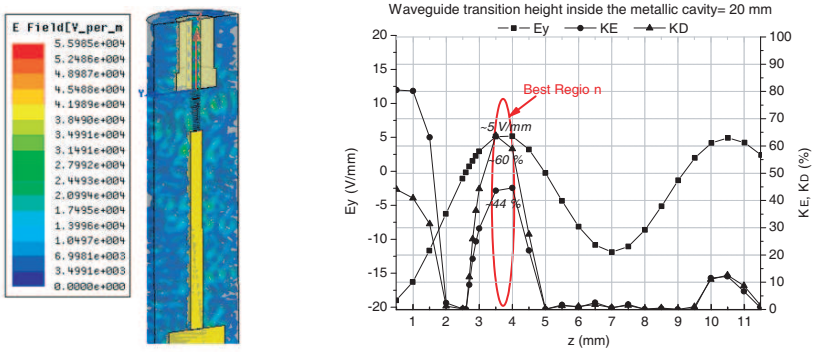

(a) (b)

Figure 7. (a) 3D plot of the magnitude of the total electric field in V/m inside the closed metallic cavity. (b) E_y, K_E and K_D calculated on the rectangles representing the sample at different positions (Model 3).

In each simulation model, we do not search for the maximum values of each descriptor separately; but we try to determine a region where there are high values of the three descriptors; E_y, K_E and K_D. Thus, the sample can be put in the chosen region which guarantees generating high Ratchet photovoltage and uniformly distributed electric field on the sample surface. If many appropriate regions are found in one model, the best position is determined with respect to the complexity of the actual setup where there is a certain tolerance in moving the sample without losing the Ratchet voltage.

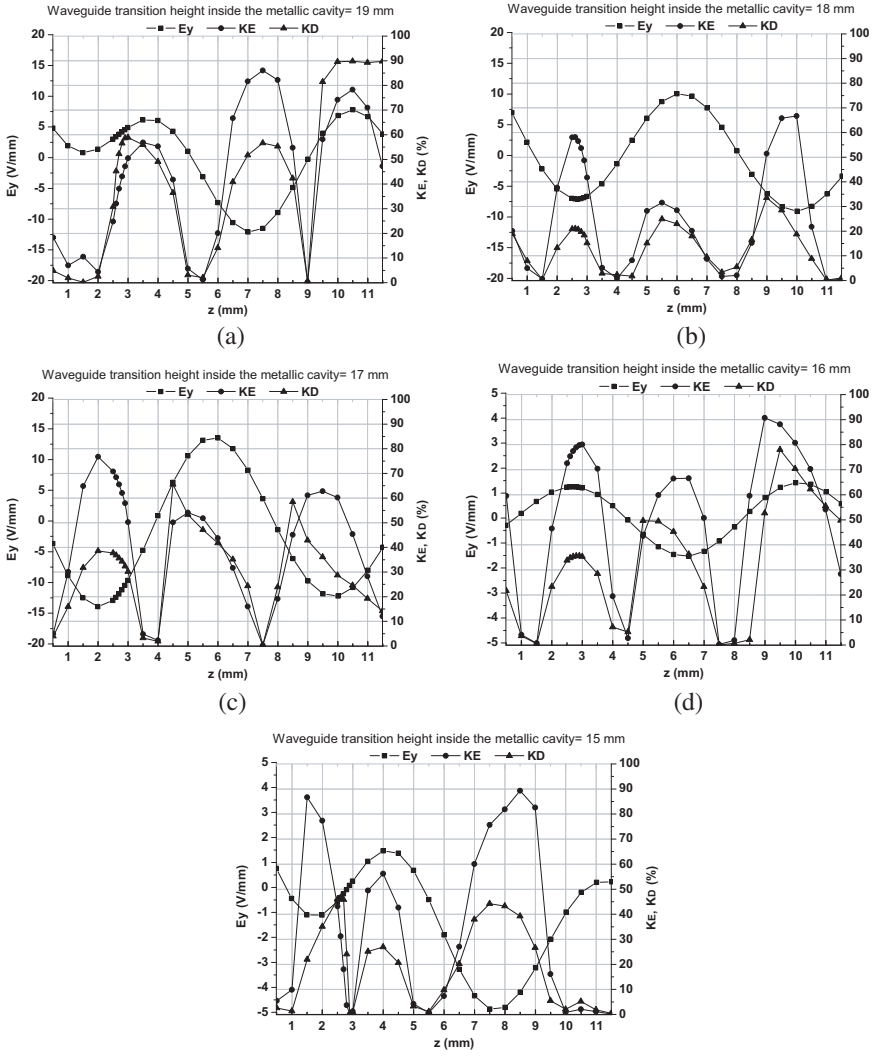

Figure 8. E_y, K_E and K_D calculated on the rectangles representing the sample at different positions when varying the waveguide transition height between 15 mm and 19 mm.

The simulation results of Model 0 in Figure 4 show that the best region where to put the sample is between 6.5 mm and 8.5 mm away from the waveport. When adding the rotating metallic cylinder, Model 1, the value of the electric field is affected. It is clear from Figure 5 that this value is decreased by 87% compared to Model 0. Also, the best

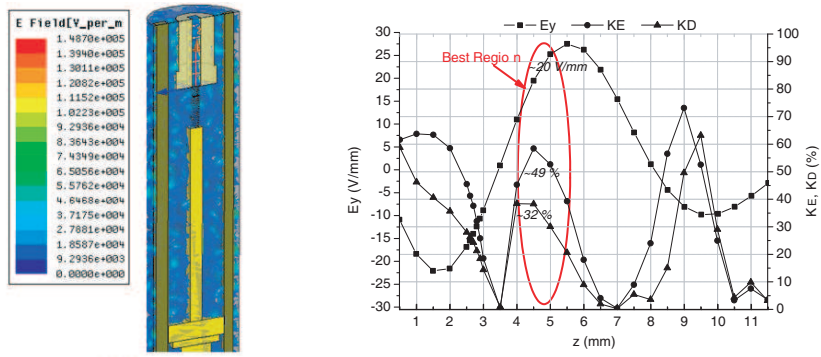

(a) (b)

Figure 9. (a) 3D plot of the magnitude of the total electric field in V/m inside the closed metallic cavity. (b) E_y, K_E and K_D calculated on the rectangles representing the sample at different positions (Model 4).

region in this model is shifted between 3 mm and 5 mm. For Model 2, 50% of the electric field is lost compared to Model 1. In this model, the sample can be placed between 4.5 mm and 6 mm, as it is shown in Figure 6.

When the waveguide transition penetrates the metallic cavity of the setup with a height of 20 mm, Model 3, the best region becomes too narrow compared to the previous models. From Figure 7, the sample can only be placed between 3.5 mm and 4 mm which means that there is a tight tolerance of 0.5 mm. Therefore, a parametric study of the transition height inside the cavity is performed. The rectangles representing the sample remain at fixed position while decreasing the transition height by 1 mm. The results presented in Figure 8 demonstrate that the three descriptors are improved if the transition height is 19 mm instead of 20 mm used in the actual setup. The best region is between 6.5 mm and 8 mm. These last results show how a little change in the transition height can totally change the electromagnetic behavior of the setup.

Finally, Figure 9 presents the simulation results of Model 4 which is the most complex model. As described in Section 3, there are four cylindrical metallic tubes in the actual experimental setup. Due to the memory limitation, only two cubical metallic tubes are simulated to estimate the setup response when adding metallic parts near the cavity boundary. The results are enhanced compared to Model 3 and the best region is located between 4 mm and 5.5 mm. The convergence criteria used in simulating these models are: maximum delta S is

0.01 and the minimum number of converged passes is 3. However due to the complexity of Model 4, the criteria used are 0.05 and 2 respectively. The maximum delta S is defined as the maximum change in the magnitude of the S-parameters between two consecutive passes.

6. CONCLUSION

In this paper, a detailed methodology has been presented to optimize the experimental setup used in controlling the Ratchet Effect. Many electromagnetic simulation models have been created to demonstrate that each metallic part added to the setup has a great influence on the electromagnetic behavior of the whole system. It has been noticed that in every model there is an optimal region where it is preferable to place the sample. This region changes its position according to the metallic parts added to the system. Its range is about 1.5 mm which means that a little change in the sample position, changes the experimental results obtained. From the simulation results of Model 4, which is the closest model to the actual setup, it is better to put the sample between 4 mm and 5.5 mm if a 20 mm transition height is used.

We have proposed a general methodology that can be used when observing a physical phenomenon which requires using a cryogenic metallic closed system and microwave radiation. Optimizing the experimental setup allows us to develop good current generators and detectors in the GHz and the THz range. The Ratchet device will make a real challenge in the wireless communication domain.

ACKNOWLEDGMENT

This work has been supported by the French Research Agency under project NANOTERRA ANR-08-NANO-018. The authors acknowledge the contribution of J.-C. Portal, E. S. Kannan and I. Bisotto in the development of the experimental setup and for the useful discussions.

REFERENCES

1. Feynman, R. P., Leighton, and M. Sands, *The Feynman Lectures on Physics*, Vol. 1, Ch. 46, Addison Wesley, 1963.
2. Sassine, S., "Transport électronique contrôlé par micro-ondes dans des microstructures asymétriques: Effet ratchet mésoscopique," Ph.D. Dissertation, University Toulouse, France, 2007.
3. Sassine, S., Y. Krupko, J.-C. Portal, Z. D. Kvon, R. Murali, K. P. Martin, G. Hill, and A. D. Wieck, "Experimental

investigation of the ratchet effect in a two-dimensional electron system with broken spatial inversion symmetry," *Phys. Rev. B*, Vol. 78, No. 4, 045431.1–045431.5, 2008.

4. Sassine, S., Y. Krupko, E. B. Olshanetsky, Z. D. Kvon, J. C. Portal, J. M. Hartmann, and J. Zhang, "Microwave radiation induced collective response in Si/SiGe heterostructures with a 2D electron gas," *Solid State Communications*, Vol. 142, No. 11, 631–633, 2007.
5. Bisotto, I., E. S. Kannan, S. Sassine, R. Murali, T. J. Beck, L. Jalabert, and J.-C. Portal, "Microwave based nanogenerator using the ratchet effect in Si/SiGe heterostructures," *Nanotechnology Journal*, Vol. 22, No. 24, 245401.1–245401.6, 2011.
6. Kannan, E. S., I. Bisotto, J.-C. Portal, R. Murali, and T. J. Beck, "Photovoltage induced by ratchet effect in Si/SiGe heterostructures under microwave irradiation," *Appl. Phys. Lett.*, Vol. 98, No. 19, 193505.1–193505.3, 2011.
7. Chepelianskii, A. D., M. V. Entin, L. I. Magarill, and D. L. Shepelyansky, "Photogalvanic current in artificial asymmetric nanostructures," *Eur. Phys. J. B*, Vol. 56, No. 4, 323–333, 2007.
8. Drexler, C., V. V. Bel'kov, B. Ashkinadze, P. Olbrich, C. Zoth, V. Lechner, Y. V.Terent'ev, D. R. Yakovlev, G. Karczewski, T. Wojtowicz, D. Schuh, W. Wegscheider, and S. D. Ganichev, "Spin polarized electric currents in semiconductor heterostructures induced by microwave radiation," *Appl. Phys. Lett.*, Vol. 97, No. 18, 182107.1–182107.3, 2010.
9. Weber, W., L. E. Golub, S. N. Danilov, J. Karch, C. Reitmaier, B. Wittmann, V. V. Bel'kov, E. L. Ivchenko, Z. D. Kvon, N. Q. Vinh, A. F. G. van der Meer, B. Murdin, and S. D. Ganicheva, "Quantum ratchet effects induced by terahertz radiation in GaN-based two-dimensional structures," *Phys. Rev. B*, Vol. 77, No. 24, 245304.1–245304.12, 2008.
10. Olbrich, P., E. L. Ivchenko, R. Ravash, T. Feil, S. D. Danilov, J. Allerdings, D. Weiss, D. Schuh, W. Wegscheider, and S. D. Ganichev, "Ratchet Effects induced by terahertz radiation in heterostructures with a lateral periodic potential," *Phys. Rev. Lett.*, Vol. 103, No. 9, 090603.1–090603.4, 2009.
11. Chepelianskii, A. D. and D. L. Shepelyansky, "Directing transport by polarized radiation in the presence of chaos and dissipation," *Phys. Rev. B*, Vol. 71, No. 5, 052508.1–052508.4, 2005.
12. Chepelianskii, A. D., M. V. Entin, L. I. Magarill, and D. L. Shepelyansky, "Ratchet transport of interacting particles," *Phys. Rev. E*, Vol. 78, No. 4, 041127.1–041127.8, 2008.

13. Ait-Haddou, R. and W. Herzog, "Brownian Ratchet models of molecular motors," *Cell Biochemistry and Biophysics*, Vol. 38, No. 2, 191–213, 2003.
14. Linke, H., B. J. Aleman, L. D. Melling, M. J. Taormina, M. J. Francis, C. C. Dow-Hygelund, V. Narayanan, P. Taylor, and A. Stout, "Self-propelled leidenfrost droplets," *Phys. Rev. Lett.*, Vol. 96, No. 15, 154502.1–154502.4, 2006.
15. Song, A. M., "Electron ratchet effect in semiconductor devices and artificial materials with broken centrosymmetry," *Appl. Phys. A*, Vol. 75, No. 2, 229–235, 2002.
16. Medhat, D., A. Takacs, and H. Aubert, "Optimum position of the two-dimensional electron gas sample in the cryogenic metallic cavity system used in studying Ratchet Effect," *Proceedings of the European Microwave Conference EuMC*, 964–967, Manchester, Oct. 2011.
17. Ansoft HFSS v.12, www.ansoft.com.
18. Medhat, D., A. Takacs, H. Aubert, and J.-C. Portal, "Comparative analysis of different techniques for controlling Ratchet Effect in a periodic array of asymmetric antidots," *Proceedings of the Asia Pacific Microwave Conference APMC*, 1711–1714, Singapore, Dec. 2009.
19. Takacs, A., D. Medhat, H. Aubert, and J. C. Portal, "Electromagnetic analysis of the experimental setup used to investigate the Ratchet Effect in two-dimensional electron system under microwave radiation," *Proceedings of the International Semiconductor Conference CAS*, Vol. 1, No. 10, 337–340, Sinaia, Oct. 2009.
20. Takacs, A., D. Medhat, H. Aubert, and J.-C. Portal, "A method for estimating the electromagnetic power delivered by the front-end module used to investigate the Ratchet Effect in two-dimensional electron gas system under microwave radiation," *Proceedings of the European Microwave Conference EuMC*, 1560–1563, Paris, Sep. 2010.
21. Medhat, D., A. Takacs, H. Aubert, and J.-C. Portal, "Investigation of the metallic cavity influence on the electromagnetic behavior of the setup used in studying the ratchet effect," *Progress In Electromagnetics Research Symposium Abstracts*, 452–453, Marrakesh, Morocco, Mar. 20–23, 2011.